Limit of Doppler cooling

Y. Castin, H. Wallis,* and J. Dalibard

Laboratoire de Spectroscopie Hertzienne de l'Ecole Normale Supérieure et Collège de France, 24 rue Lhomond, 75231 Paris Cedex 05, France

Received April 3, 1989; accepted June 15, 1989

We present a quantum theory of one-dimensional laser cooling of free atoms using a transition with a $J = 0$ ground state and a $J = 1$ excited state. This treatment is valid both for broad lines (recoil energy small compared with the energy width $\hbar\Gamma$ of the excited level) and for narrow lines. For broad lines we recover the well-known cooling limit for a two-level transition ($\sim\hbar\Gamma/2$), whereas for a narrow line the cooling limit is found to be of the order of the recoil energy. The stationary momentum distribution is obtained for both cases and is found to be close to the one obtained by Monte Carlo simulations.

1. INTRODUCTION

Laser cooling of free atoms is a technique that has been widely investigated both theoretically and experimentally during the past several years. The simplest cooling mechanism is the so-called Doppler cooling initially proposed by Hänsch and Schawlow for free atoms[1] and by Wineland and Dehmelt for trapped particles.[2] Doppler cooling occurs when atoms are irradiated with counterpropagating laser waves detuned below resonance. Owing to the Doppler effect, a moving atom will tend to absorb photons into the laser wave counterpropagating its velocity rather than into the copropagating wave; thus it encounters a force opposed to its velocity and becomes cooled.

The purpose of this paper is to study the Doppler-cooling mechanism and its limits by a fully quantum treatment of atomic motion. Until now, Doppler cooling was investigated mainly by using a semiclassical treatment of the atom–laser interaction.[3] Such a treatment is valid for broad atomic lines—the energy width of the excited state $\hbar\Gamma$ is large compared with the recoil energy $E_r = \hbar^2k^2/2m$—and leads to the well-known cooling limit for two-level atoms[3]

$$\bar{E}_k = \frac{1}{2}m\overline{\mathbf{v}^2} \simeq \frac{1}{4}\hbar\Gamma \gg E_r = \frac{\hbar^2k^2}{2m}. \tag{1.1}$$

The residual kinetic energy $\bar{E}_k$ is of the order of $\hbar\Gamma$, and it is therefore large compared with the recoil energy. Much less work has been devoted to the problem of Doppler cooling with narrow atomic lines ($E_r \gtrsim \hbar\Gamma$) for which a semiclassical treatment is no longer valid: Such a treatment indeed requires that the atomic position be known to an uncertainty Δx much smaller than λ (scale of variation of the laser field) and also that the atomic velocity be known such that the uncertainty $k\Delta v$ on the Doppler shift is smaller than the natural width Γ of the excited state.[4] For a narrow line, the Heisenberg uncertainty relation prevents these two conditions from being fulfilled simultaneously. By contrast, a fully quantum treatment should allow the two regimes of Doppler cooling (broad or narrow lines) to be connected together.

Experimentally, the measured temperatures of laser-cooled atoms in the so-called optical molasses[5] were recently shown to be much lower than the limit given in expression (1.1), even for broad atomic transitions.[6–8] This is probably due to the multilevel structure of the atomic ground state involved in the process.[7,8] This structure leads to extra cooling via the polarization gradient force, which is in addition to the previously described Doppler cooling. Here, we do not wish to investigate this new cooling regime; therefore we focus on a transition involving a nondegenerate $J_g = 0$ ground state and a $J_e = 1$ excited state. We note, however, that our quantum treatment can also be generalized to more-complicated atomic transitions. Thus it can be a starting point in the investigation of the limits of the newly discovered extra cooling that seems to approach the recoil limit[9] and therefore may also require a quantum treatment.[10]

Here we focus on the one-dimensional cooling of $J_g = 0$, $J_e = 1$ atoms, irradiated by two counterpropagating σ_+ and σ_- polarized plane waves, respectively (Fig. 1). This schematic is already known to be simpler than that of a two-level atom in a standing wave.[11] In the latter case, coherent redistribution of photons may indeed occur between the two waves by absorption in one wave and stimulated emission in the other wave. In the σ_+–σ_- configuration, conservation of angular momentum prevents such a redistribution from occurring.

Here we use the method of families first presented in Refs. 12 and 13. This method recently was applied to the study of cooling below the recoil energy, using coherent population trapping.[14] The principle of the method for the present case is as follows: If we consider for any momentum p the family formed by the three states $|g, p\rangle$, $|e_+, p + \hbar k\rangle$, $|e_-, p - \hbar k\rangle$, we find that this family remains globally invariant in the evolution resulting from the kinetic-energy term and the laser–atom interaction term of the total Hamiltonian. Connections among various families are caused only by spontaneous emission and are easy to handle. Once these concepts have been precisely defined (Section 2), we turn to the time evolution and to the stationary solution for the atomic density matrix (Sections 3 and 4). We find, in particular, that for a narrow line the stationary solution for $W(p)$, the probability for finding the atom with momentum p, may be far from a Gaussian, contrary to the broad-line result. Finally, we

0740-3224/89/112046-12$02.00

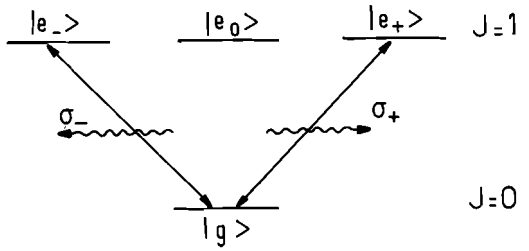

Fig. 1. A $(g, J = 0) \rightarrow (e, J = 1)$ atom irradiated by two counterpropagating σ_+ and σ_- polarized waves.

consider specifically weak excitations (Rabi frequency $\Omega \ll \Gamma$) for which it is possible to obtain an analytical derivation of various averages $\langle p^n \rangle$ in the stationary state. In particular, we show that for very narrow lines, the smallest rms momentum $\sqrt{\langle p^2 \rangle}$ is reached for a detuning δ between the laser frequency ω_L and the atomic frequency ω_A such that

$$\delta = \omega_L - \omega_A \simeq -1.7 \frac{\hbar k^2}{m}, \tag{1.2}$$

leading to

$$\bar{E}_k = \frac{\overline{p^2}}{2m} \simeq 0.5 E_r \gg \hbar\Gamma. \tag{1.3}$$

Now let us discuss briefly how our work ties in with previous results. In Ref. 15, Wineland and Itano considered the problem of laser cooling with narrow atomic lines but used a different hypothesis: They assumed they had a collection of atoms in which collisions would ensure complete thermalization between two successive photon-scattering processes so that the velocity distribution would be Gaussian at any time. In their model, they could then reach a temperature well below the recoil energy E_r. By contrast, we consider here a single atom, and we do not make any hypothesis about the momentum distribution. The recoil energy can then be shown to be a natural lower bound to energies accessible by Doppler cooling.[16]

Recently, Wallis and Ertmer did a study of laser cooling using a narrow atomic line and a broadband laser.[17] This technique ensured that, in spite of the narrowness of the atomic line, the atom was always resonant with one of the two counterpropagating laser beams. They obtained a minimum residual kinetic energy of the order of $\hbar\Gamma$, well below the single-line limit found here [Eq. (1.3)]. This technique therefore appears to be quite promising, provided that the proposed multiline spectrum can be realized.[18]

Recently as well, W. Phillips and co-workers performed a Monte Carlo simulation of three-dimensional Doppler cooling, using both narrow atomic and laser lines.[19] Their results appear to be close to the ones that we obtained with the quantum model.

2. MOMENTUM FAMILIES AND THEIR EVOLUTION

A. Definition of Momentum Families

As we noted in the Introduction, the choice of a σ_+–σ_- laser configuration leads to a simple structure for the atomic evolution equations. Consider, for example, the state $|g, p\rangle$ (atom in the ground state with momentum $p_z = p$ along the axis Oz of propagation of the laser beam). This state is coupled to two other states $|e_+, p + \hbar k\rangle$ and $|e_-, p - \hbar k\rangle$ by absorption of σ_+ or σ_- laser photon. Because of conservation of angular momentum, these two states are themselves coupled only to $|g, p\rangle$ by stimulated-emission processes. We are then led to consider, for any momentum p, the family $\mathcal{F}(p)$ formed by the three states:

$$\mathcal{F}(p) = \{|g, p\rangle, |e_+, p + \hbar k\rangle, |e_-, p - \hbar k\rangle\}. \tag{2.1}$$

Using this basis, we can expand the atomic density operator ρ. In particular, we put

$$\begin{aligned}
\pi_g(p) &= \langle g, p|\rho|g, p\rangle, \\
\pi_+(p) &= \langle e_+, p + \hbar k|\rho|e_+, p + \hbar k\rangle, \\
\rho_{g_+}(p) &= \langle g, p|\rho|e_+, p + \hbar k\rangle \exp(-i\omega_L t), \\
\rho_{+-}(p) &= \langle e_+, p + \hbar k|\rho|e_-, p - \hbar k\rangle,
\end{aligned} \tag{2.2}$$

and the five quantities deduced by exchanging + and − and by taking complex conjugates.

At first sight, the knowledge of these nine quantities for any momentum p is not sufficient to determine completely the atomic density operator ρ. However, we see in what follows that this set of nine functions of p is closed with respect to the time evolution in the case of a $\sigma_+ - \sigma_-$ laser configuration: None of the time derivatives $\dot{\pi}_g$, $\dot{\rho}_{g+}$, ... involves any coupling to interfamily density-matrix elements, such as $\langle g, p|\rho|g, p'\rangle$ with $p \neq p'$; i.e., matrix elements of the density operator ρ between a bra and a ket belonging to two different families $\mathcal{F}(p)$ and $\mathcal{F}(p')$.

One should be aware that the quantity p is just the label of the family and not necessarily the atomic momentum. For example, $\pi_+(p)$ denotes the probability of finding the atom in the internal state $|e_+\rangle$ with momentum $p + \hbar k$. For the ground state, however, p coincides with the expected atomic momentum.

One can also note that definitions (2.2) are monodimensional. Actually, one must consider them as traces over the two axes Ox and Oy, so that one has, for instance,

$$\begin{aligned}
\pi_g(p) &= \langle g, p|\rho|g, p\rangle \\
&= \int\int_{-\infty}^{+\infty} dp_x dp_y \langle g, p_x, p_y, p_z = p|\rho|g, p_x, p_y, p_z = p\rangle.
\end{aligned} \tag{2.3}$$

This trace over p_x and p_y plays an important role in the description of spontaneous-emission processes (see Appendix A).

We now consider the evolution of the atomic density matrix using this family basis. This evolution contains three terms: a term resulting from the atomic kinetic energy and internal energy

$$H_0 = \frac{P_z^2}{2m} + \hbar\omega_A \sum_{i=0,+,-} |e_i\rangle\langle e_i|; \tag{2.4}$$

a term resulting from the atom–laser coupling, which we take here in the electric-dipole and rotating-wave approximations,

$$V = -[\mathbf{D}^+ \cdot \mathcal{E}^+(Z)\exp(-i\omega_L t) + \mathbf{D}^- \cdot \mathcal{E}^-(Z)\exp(i\omega_L t)]; \tag{2.5}$$

and a term resulting from spontaneous emission. In Eq. (2.5), $\mathbf{D}^+$ and $\mathbf{D}^-$ are the raising and lowering parts of the atomic-dipole operator, $\mathcal{E}^+$ and $\mathcal{E}^-$ are the positive- and negative-frequency parts of the (classical) laser electric field, and Z is the atomic position operator along the Oz axis.

B. Evolution from the Atomic Internal Energy and Kinetic Energy

The evolution resulting from H_0 does not modify the value of the populations π_g, π_+, π_- since $|g, p\rangle$, $|e_\pm, p \pm \hbar k\rangle$ are eigenstates of H_0. For the optical coherences ρ_{+g}, ρ_{-g}, ... we find, by including the derivative of their explicit time dependence $e^{(\pm i\omega_L t)}$, that

$$[\dot{\rho}_{g+}(p)]_{H_0} = -i\left(\omega_L - \omega_A - \frac{kp}{m} - \frac{\hbar k^2}{2m}\right)\rho_g + (p). \tag{2.6}$$

$\rho_{g+}(p)$ then oscillates at a frequency equal to the bare detuning

$$\delta = \omega_L - \omega_A \tag{2.7}$$

modified by both the Doppler shift $-kp/m$ and the recoil shift $-\hbar k^2/2m$. In what follows, we introduce the renormalized detuning $\bar{\delta}$, which includes the recoil shift

$$\bar{\delta} = \omega_L - \omega_A - \frac{\hbar k^2}{2m}. \tag{2.8}$$

Finally, the evolution from H_0 of the excited-state coherences ρ_{+-} and ρ_{-+} is given by

$$[\dot{\rho}_{+-}(p)]_{H_0} = -2i\frac{kp}{m}\rho_{+-}(p),$$
$$\rho_{-+}(p) = [\rho_{+-}(p)]^*. \tag{2.9}$$

C. Evolution from Atom–Laser Coupling

The atom–laser coupling has been given in Eq. (2.5). In this equation, the atomic-dipole operators can be written as

$$\mathbf{D}^- = d(|g\rangle\langle e_+|u_+ + |g\rangle\langle e_-|u_- + |g\rangle\langle e_0|u_z),$$
$$\mathbf{D}^+ = (\mathbf{D}^-)^+, \tag{2.10}$$

d is the atomic-dipole constant, u_z is a unit vector along Oz, and u_+ and u_- are the unit vectors corresponding to σ_+ and σ_- polarizations along Oz:

$$u_+ = -\frac{1}{\sqrt{2}}(u_x + iu_y),$$
$$u_- = \frac{1}{\sqrt{2}}(u_x - iu_y). \tag{2.11}$$

The laser electric fields $\mathcal{E}^+(Z)$ and $\mathcal{E}^-(Z)$, resulting from the superposition of the σ_+ wave and σ_- wave with wave vectors equal to $k\,u_z$ and $-k\,u_z$, respectively, can be written as

$$\mathcal{E}^+(Z) = \frac{\mathcal{E}_0}{2}(u_+ e^{ikz} + u_- e^{-ikz}),$$
$$\mathcal{E}^-(Z) = [\mathcal{E}^+(Z)]^+, \tag{2.12}$$

where $\mathcal{E}_0$ is the field amplitude of each of the traveling waves. We now introduce the atom–laser field coupling constant (Rabi frequency for each traveling wave):

$$\Omega = -\frac{d\mathcal{E}_0}{\hbar}, \tag{2.13}$$

and, using

$$e^{ikz}|p\rangle = |p + \hbar k\rangle, \tag{2.14}$$

we get

$$V|g, p\rangle = \frac{\hbar\Omega}{2}(|e_+, p + \hbar k\rangle + |e_-, p - \hbar k\rangle),$$
$$V|e_\pm, p \pm \hbar k\rangle = \frac{\hbar\Omega}{2}|g, p\rangle, \tag{2.15}$$

where we assumed that Ω is real.

We now calculate the equations of evolution resulting from the laser of the density matrix:

$$[\dot{\pi}_+(p)]_V = \frac{i\Omega}{2}[\rho_{+g}(p) - \rho_{g+}(p)],$$
$$[\dot{\pi}_g(p)]_V = -\frac{i\Omega}{2}[\rho_{+g}(p) - \rho_{g+}(p)] - \frac{i\Omega}{2}[\rho_{-g}(p) - \rho_{g-}(p)],$$
$$[\dot{\rho}_{g+}(p)]_V = \frac{i\Omega}{2}[\pi_g(p) - \pi_+(p)] - \frac{i\Omega}{2}\rho_{-+}(p),$$
$$[\dot{\rho}_{+-}(p)]_V = \frac{i\Omega}{2}[\rho_{+g}(p) - \rho_{g-}(p)]. \tag{2.16}$$

The five other equations for π_-, ρ_{+g}, ρ_{g-}, ρ_{-g}, and ρ_{-+} can be deduced from these four by taking complex conjugates and exchanging + and −.

D. Evolution from Spontaneous Emission

We now come to the evolution of the atomic density operator from spontaneous-emission processes. The structure of the resulting terms, expressed in the momentum family basis, is more complicated than the previous contributions. A given family is indeed not invariant under spontaneous-emission processes. For example, the quantity $\pi_g(p) = \langle g, p|\rho|g, p\rangle$, representing the population of the ground state g with momentum p, can be fed by any $\langle e_+, p'|\rho|e_+, p'\rangle = \pi_+(p' - \hbar k)$, provided that p' and p differ by less than $\hbar k$. In Appendix A we show that

$$[\dot{\pi}_g(p)]_{SE} = \Gamma\int_{-\hbar k}^{\hbar k} dp' \mathcal{N}(p')[\pi_+(p + p' - \hbar k) + \pi_-(p + p' + \hbar k)]$$
$$= \Gamma[\bar{\pi}_+(p - \hbar k) + \bar{\pi}_-(p + \hbar k)], \tag{2.17}$$

where $\mathcal{N}(p')dp'$ is the probability that when a fluorescence photon circularly polarized along Oz is emitted it will have its momentum along z between p' and $p' + dp'$ (dipole radiation pattern):

$$\mathcal{N}(p') = \frac{3}{8\hbar k}\left(1 + \frac{p'^2}{\hbar^2 k^2}\right), \tag{2.18}$$

and where the functions $\bar{\pi}_\pm$ are defined by

$$\bar{\pi}_\pm(p) = \int_{-\hbar k}^{\hbar k} dp' \mathcal{N}(p')\pi_\pm(p + p'). \tag{2.19}$$

The evolution of the eight other family quantities defined in Eqs. (2.2) is much simpler, corresponding simply to the usual decrease resulting from spontaneous emission. One has, for example,

$$[\dot{\pi}_+(p)]_{SE} = -\Gamma\pi_+(p),$$
$$[\dot{\rho}_{+-}(p)]_{SE} = -\Gamma\rho_{+-}(p), \tag{2.20}$$
$$[\dot{\rho}_{g+}(p)]_{SE} = -\frac{\Gamma}{2}\rho_{g+}(p).$$

E. Structure of the Equations of Evolution

If one puts together all the various terms found above, one gets

$$\dot{\pi}_g(p) = \Gamma[\bar{\pi}_+(p-\hbar k) + \bar{\pi}_-(p+\hbar k)] - \frac{i\Omega}{2}[\rho_{+g}(p) - \rho_{g+}(p)] - \frac{i\Omega}{2}[\rho_{-g}(p) - \rho_{g-}(p)],$$

$$\dot{\pi}_+(p) = -\Gamma\pi_+(p) + \frac{i\Omega}{2}[\rho_{+g}(p) - \rho_{g+}(p)],$$

$$\dot{\rho}_{g+}(p) = -\left[i\left(\bar{\delta} - \frac{kp}{m}\right) + \frac{\Gamma}{2}\right]\rho_{g+}(p) + \frac{i\Omega}{2}[\pi_g(p) - \pi_+(p)] - \frac{i\Omega}{2}\rho_{-+}(p),$$

$$\dot{\rho}_{+-}(p) = -\left(2i\frac{kp}{m} + \Gamma\right)\rho_{+-}(p) + \frac{i\Omega}{2}[\rho_{+g}(p) - \rho_{g-}(p)], \tag{2.21}$$

plus the five equations that can be deduced from Eqs. (2.21) by taking complex conjugates and/or exchanging + and −.

Let us comment briefly on the structure of these equations. A first important remark is that the evolution of any of the nine functions $\pi_g(p)$, $\pi_+(p)$, $\rho_{+g}(p)$, ... does not involve any coupling to interfamily density-matrix elements such as $\langle g, p|\rho|g, p'\rangle$ with $p \neq p'$. This simplification, which we mentioned at the beginning of this section, arises from the choice of a σ_+–σ_- laser configuration. The conservation of angular momentum in this case prevents any coherent redistribution of photons between the two counterpropagating waves from taking place, which would in turn couple these nine functions to the interfamily density-matrix elements. This simplification must be contrasted with the case of a two-level atom in a standing wave. In the latter case, one finds that the state $|g, p\rangle$ is coupled by absorption from a traveling wave to the state $|e, p + \hbar k\rangle$, itself coupled by stimulated emission into the other traveling wave to $|g, p + 2\hbar k\rangle$, and so on .... The quantum treatment of this problem would then require consideration of, for instance, an infinite number of elements $\langle g, p|\rho|g, p'\rangle$ with $|p' - p| = 2n\hbar k$, instead of keeping only $\langle g, p|\rho|g, p\rangle$. Actually, at low power (Rabi frequency Ω smaller than the width Γ), we do not expect a large difference between the σ_+–σ_- configuration and the standing-wave case, since stimulated processes are negligible compared with spontaneous ones. On the other hand, at high power ($\Omega \gg \Gamma$), we know from the semiclassical treatment that the two configurations lead to quite different results.[11]

With regard to the structure of the equations of evolution (2.21), we also can note that all these equations except for the one giving $\dot{\pi}_g$ are similar to usual optical Bloch equations, the label p being just a spectator. On the other hand, the equation giving $\pi_{\dot{g}}$ contains the term $\Gamma(\bar{\pi}_+ + \bar{\pi}_-)$, which describes the transfer among families because of recoil. This term is at the origin of the radiation force and its fluctuations.[12] Now if we consider the evolution of the total population of the family p, we get

$$\dot{\pi}_g(p) + \dot{\pi}_+(p) + \dot{\pi}_-(p) = -\Gamma[\pi_+(p) + \pi_-(p)] + \Gamma[\bar{\pi}_+(p-\hbar k) + \bar{\pi}_-(p+\hbar k)]. \tag{2.22}$$

This equation has a clear physical meaning: The atom leaves the family p by spontaneous emission from level $|e_+, p + \hbar k\rangle$ and $|e_-, p - \hbar k\rangle$ {terms $-\Gamma[\pi_+(p) + \pi_-(p)]$}, and it enters this family by spontaneous emission from any $|e_\pm, p'\rangle$ with $|p' - p| \leqslant \hbar k$ (terms involving $\bar{\pi}_+$ and $\bar{\pi}_-$). When stationary state is reached, these two entering and leaving fluxes are equal for any family p.

3. NUMERICAL RESULTS FOR ARBITRARY INTENSITIES

In order to study the dynamics and the stationary state of the atomic density matrix, we performed a numerical study of the full set of Eqs. (2.21). We discretized the momenta by using typically 200 points. For a narrow line (Fig. 2) corresponding to $\hbar\Gamma = E_r$, we took 10 points per recoil $\hbar k$. In comparison, numerical solutions of the usual Fokker–Planck approach involve typically one point per recoil $\hbar k$.

In Fig. 2, we plotted for this narrow line the evolution of the function giving the probability $W(p)$ of finding the atom with a momentum p, independently of its internal state

$$W(p) = \pi_g(p) + \pi_+(p - \hbar k) + \pi_-(p + \hbar k). \tag{3.1}$$

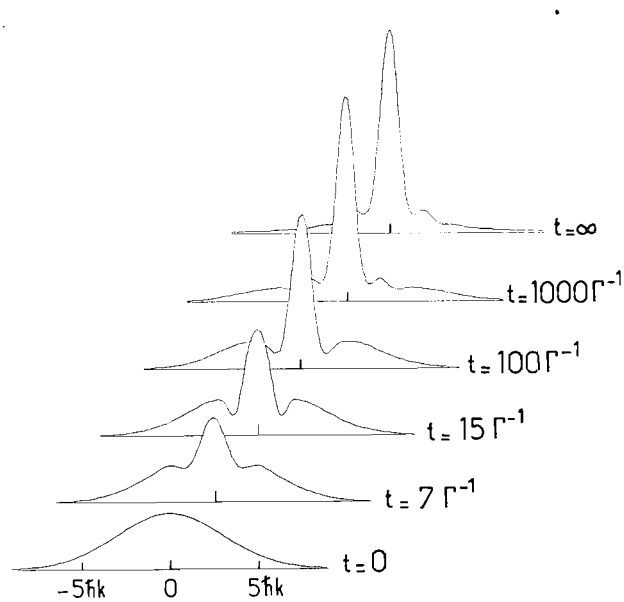

Fig. 2. Time evolution of the momentum distribution $W(p)$ for the case of a narrow line ($\hbar\Gamma = E_r$) with a Rabi frequency $\Omega = \Gamma$ and a detuning $\bar{\delta} = -2.5\Gamma$ (discretization 200 points, 10 points per recoil momentum). The last distribution (for $t = \infty$) was obtained directly by solving the set of equations deduced from $\dot{\rho} = 0$.

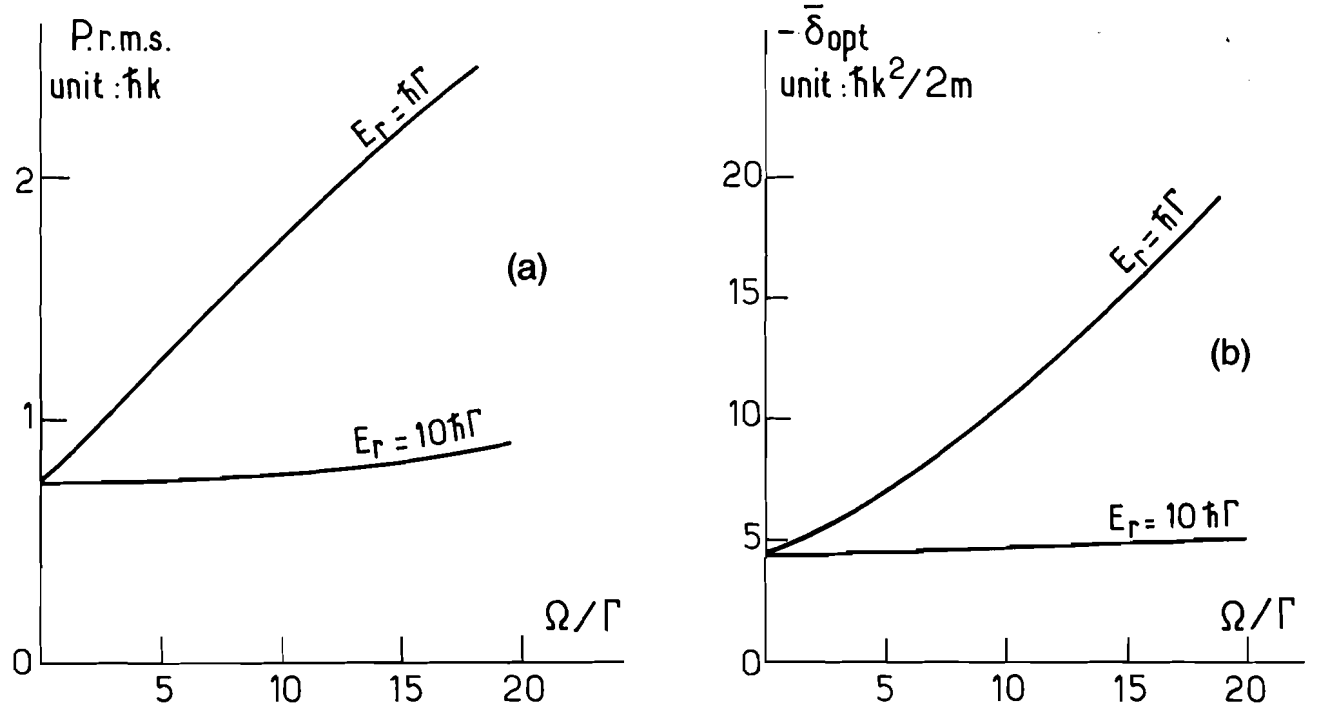

Fig. 3. (a) Variation of the stationary rms momentum with Rabi frequency Ω for the two narrow lines $\hbar\Gamma = E_r$ and $\hbar\Gamma = 0.1E_r$. For each Rabi frequency we took the detuning $\bar{\delta}$ that minimizes the rms momentum. (b) Variation with the Rabi frequency Ω of the detuning $\bar{\delta}$ that minimizes the rms momentum for the two lines $\hbar\Gamma = E_r$ and $\hbar\Gamma = 0.1E_r$.

The distribution $W(p)$ in the stationary state exhibits a triplet structure, with local minima at the resonant momenta. The stationary state was obtained consistently by looking for the long-time limit of the time-dependent solution of Eqs. (2.21) and directly solving the set of equations deduced from Eqs. (2.21) by setting $\dot{\rho} = 0$ and $\mathrm{Tr}\,\rho = 1$.

We then calculated for the stationary state the value of the rms momentum, which is an indicator of the quality of cooling. Note that, for narrow lines, there is no equivalent of a temperature any more since the momentum distribution is not Maxwellian. We have always found that the lowest rms momenta are obtained at low power ($\Omega \ll \Gamma$). As an example, we plotted in Fig. 3(a), for the two lines $\hbar\Gamma = E_r$ and $\hbar\Gamma = E_r/10$, the minimum rms momentum as a function of the Rabi frequency Ω. The detuning $\bar{\delta}$ is optimized for each value of Ω in order to minimize the rms momentum [see Fig. 3(b)]. In Fig. 4, we have plotted for the line $\hbar\Gamma = E_r$ some stationary momentum distributions, for a given detuning $\bar{\delta} = -1.25\hbar k^2/m$ and for various Rabi frequencies.

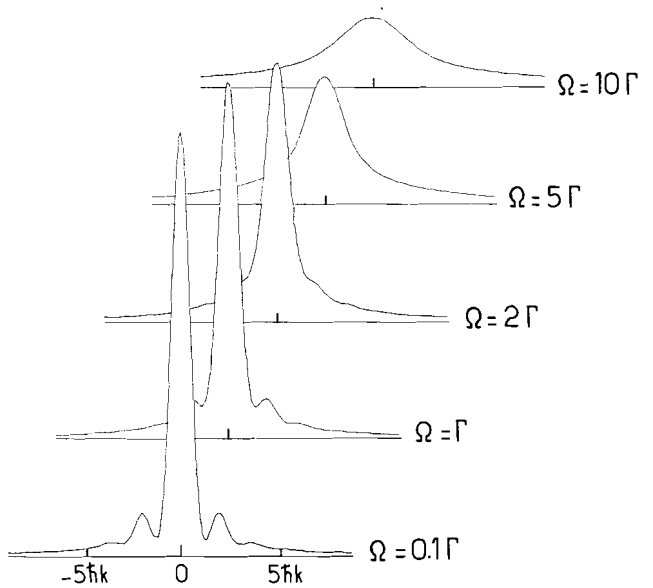

Fig. 4. Stationary momentum distributions $W(p)$ for various Rabi frequencies Ω, in the case of a narrow line $\hbar\Gamma = E_r$ ($\bar{\delta} = -2.5\Gamma$).

Restricting ourselves now to the low-power domain, we studied numerically the cooling limit as a function of the ratio $\hbar\Gamma/E_r$. For broad lines, we recovered the limit for the average kinetic energy $\bar{E}_K$:

$$\bar{E}_K \simeq \frac{7\hbar\Gamma}{40} \tag{3.2}$$

for a detuning $\bar{\delta} = -\Gamma/2$. [Let us recall that we are considering here a one-dimensional problem and are taking into account the dipole radiation pattern: The cooling limit would then be slightly different from expression (1.1).] For ultranarrow lines, the optimum detuning is $\bar{\delta} \simeq -2.2\hbar k^2/m$ and leads to the limit

$$\bar{E}_K \simeq 0.5E_r. \tag{3.3}$$

We see in Section 4 how these results can be obtained in a faster and more precise way by using analytical arguments.

We also looked for the time constants involved in the transitory regime toward the stationary state. The first way to obtain these time constants is to look for the eigenvalues of the discretized system derived from Eqs. (2.21). This

approach has led us (at low power) to the well-known time constant

$$\mathcal{C} \simeq \frac{m}{\hbar k^2}\frac{\Gamma^2}{\Omega^2} \tag{3.4}$$

for broad lines[3] and to

$$\mathcal{C} \text{ proportional to } \frac{E_r^{\,2}}{\Gamma(\hbar\Omega)^2} \tag{3.5}$$

for narrow lines. In order to understand this last result, we developed the following semiquantitative argument, which is valid at low power. We take an atom with a momentum p large compared with $\hbar k$, and we look for the average time that it takes to reach the zero momentum. The average time required to decrease this momentum p by $\hbar k$ is

$$t_p \simeq \frac{1}{\gamma_- - \gamma_+} \approx \frac{kp^3}{2\hbar\Gamma m^2\Omega^2}, \tag{3.6}$$

where γ_+ and γ_- represent the atomic excitation rates corresponding to the two traveling waves

$$\gamma_\pm = \Gamma\frac{\Omega^2/4}{(\bar{\delta} \mp kp/m)^2 + \Gamma^2/4} \tag{3.7}$$

and where we chose $\bar{\delta} = -2\hbar k^2/m$ (close to the optimal detuning for narrow lines). Summing up over the various time steps t_p, we get the order of magnitude of the average time ϕ required to decrease the momentum p to 0:

$$\begin{aligned}\phi &= t_p + t_{p-\hbar k} + t_{p-2\hbar k} + \ldots + t_{\hbar k} \\ &\simeq \frac{1}{2\Gamma}\frac{(p^2/2m)^2}{(\hbar\Omega)^2}.\end{aligned} \tag{3.8}$$

This result is clearly in agreement with the one obtained numerically [expression (3.5)]. If we choose $\Omega \simeq \Gamma$ (limit for this low-power argument), we obtain that the cooling time for narrow lines varies as Γ^{-3}.

Finally, we can say that we performed, in the low-intensity domain, a Monte Carlo simulation of this problem in a rate-equation approximation. Absorption and spontaneous-emission processes were allowed for in a random way, according to rates calculated from optical Bloch equations. The results are perfectly consistent with the fully quantum treatment (see, e.g., Fig. 5). This indicates that for the case of a narrow line the dynamics of a V system under the influence of spontaneous scattering of photons is well described in a rate-equation approach, as it is known to be the case for broad lines. This must be contrasted with the problem of a Λ system in the same σ_+–σ_- configuration, where such a rate-equation approach cannot describe the recently discovered cooling below the recoil limit by population trapping.[14]

4. LOW-INTENSITY LIMIT: AN ANALYTICAL APPROACH

In the low-intensity limit ($\Omega \ll \Gamma$), it is possible to perform an analytical study of the stationary state of equations (2.21). We derive in what follows the value of the rms momentum in the stationary state and then show how one can get an approximate analytical form for the stationary distribution $\pi_g(p)$.

A. Rms Momentum in the Low-Intensity Limit

In the low-intensity limit, one can easily extract from Eqs. (2.21) the values of $\pi_+(p)$ and $\pi_-(p)$ as functions of $\pi_g(p)$:

$$\pi_\pm(p) = \frac{\Omega^2/4}{\Gamma^2/4 + \left(\bar{\delta} \mp \dfrac{kp}{m}\right)^2}\pi_g(p). \tag{4.1}$$

This first equation relates the three populations π_+, π_-, and π_g inside a given family $\mathcal{F}(p)$. On the other hand, Eqs. (2.22) lead to

$$\pi_+(p) + \pi_-(p) = \bar{\pi}_+(p - \hbar k) + \bar{\pi}_-(p + \hbar k). \tag{4.2}$$

This second equation gives a relation among populations of

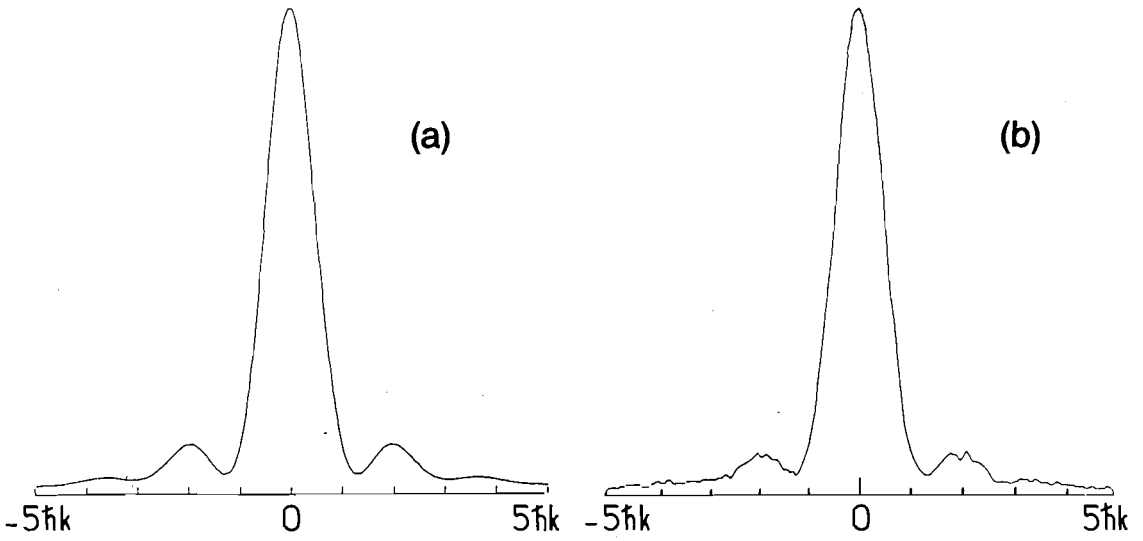

Fig. 5. Comparison of the stationary momentum distribution obtained by (a) the quantum method and (b) a Monte Carlo approach ($\hbar\Gamma = E_r$, $\Omega = 0.2\Gamma$, $\bar{\delta} = -2.5\Gamma$).

states belonging to different families. Using simultaneously the parity of the ground-state population in the stationary state

$$\pi_g(p) = \pi_g(-p), \tag{4.3}$$

it is possible then to derive all the momenta $\langle p^n \rangle$ of this stationary distribution.

First, we consider the case of a broad line ($E_r \ll \hbar\Gamma$). We multiply Eq. (4.2) by p^2 and take the integral over p from $-\infty$ to $+\infty$. We then get by using Eq. (2.19)

$$\int_{-\infty}^{+\infty} dp p^2 [\pi_+(p) + \pi_-(p)] = \int_{-\infty}^{+\infty} dp p^2 \int_{-\hbar k}^{\hbar k} dp' \mathcal{N}(p') \times [\pi_+(p + p' - \hbar k) + \pi_-(p + p' + \hbar k)]. \tag{4.4}$$

We now replace π_+ and π_- by their expression in terms of π_g [Eq. (4.1)] and take as new integration variables $p_1 = p'$ and $p_2 = p + p' \mp \hbar k$. Equation (4.4) can now be written as an average over momentum with a weight π_g:

$$\langle p(\gamma_- - \gamma_+)(p) \rangle = \frac{7}{10} \hbar k \langle (\gamma_+ + \gamma_-)(p) \rangle, \tag{4.5}$$

where the coefficients $\gamma_\pm$ are given in Eq. (3.7) and where we get from Eq. (2.18)

$$\int_{-\hbar k}^{\hbar k} dp' p'^2 \mathcal{N}(p') = \frac{2}{5} \hbar^2 k^2. \tag{4.6}$$

Relation (4.5) describes the equilibrium in the steady state between dissipation and fluctuations. The dissipation is due to the cooling force $f(p) = \hbar k(\gamma_+ - \gamma_-)(p)$, and the fluctuations are described by the momentum diffusion coefficient $7/10(\hbar k)^2(\gamma_+ + \gamma_-)(p)$. For a broad line, the average Doppler shift $|kp/m|$ in the stationary state is small compared with the natural width Γ, so that we get from Eq. (3.7)

$$\gamma_-(p) - \gamma_+(p) \simeq -\frac{\Gamma\Omega^2 \bar{\delta} kp/m}{(\bar{\delta}^2 + \Gamma^2/4)^2}, \tag{4.7}$$

$$\gamma_-(p) + \gamma_+(p) \simeq \frac{\Gamma\Omega^2/2}{\bar{\delta}^2 + \Gamma^2/4}. \tag{4.8}$$

If we insert these two results into Eq. (4.5), we get

$$\bar{E}_\kappa = \frac{\langle p^2 \rangle}{2m} = \frac{7}{40} \hbar \frac{\bar{\delta}^2 + \Gamma^2/4}{-\bar{\delta}}. \tag{4.9}$$

This is the well-known cooling limit for broad lines, which is minimum for $\bar{\delta} = -\Gamma/2$, where $\bar{E}_\kappa = 7\hbar\Gamma/40$.

For a narrow line, the problem of the derivation of $\bar{E}_\kappa$ is more complex since an expansion like the one that leads to expressions (4.7) and (4.8) is no longer possible. The principle of the calculations is presented in detail in Appendix B; here we indicate only the main results.

The first result deals with the convergence of the integral $\int_{-\infty}^{+\infty} p^{2n} \pi_g(p) dp$. We find that this integral converges if

$$\bar{\delta} < -\frac{7}{20} \frac{\hbar k^2}{m} (3 + 2n). \tag{4.10}$$

In particular, this leads to

$$\pi_g \text{ normalizable} \quad \text{if} \quad \bar{\delta} < -\frac{21}{20} \frac{\hbar k^2}{m}, \tag{4.11}$$

$$\langle p^2 \rangle \text{ exists} \quad \text{if} \quad \bar{\delta} < -\frac{7}{4} \frac{\hbar k^2}{m}. \tag{4.12}$$

Physically, this means that in an experiment with a finite collection of atoms, the number of particles with a velocity smaller than a given bound tends to zero with increasing interaction time when condition (4.11) is violated.

The analytical expression for $\langle p^2 \rangle$ is given explicitly in Appendix B [Eq. (B16)]. We plotted in Fig. 6 the variations of $\langle p^2 \rangle/2m$ with detuning δ for various ratios $\hbar\Gamma/E_r$. The optimum detunings, which minimize $\langle p^2 \rangle$, range from $\delta = -\Gamma/2$ for a broad line to $\delta = -1.72\hbar k^2/m = -3.44\Gamma(E_r/\hbar\Gamma)$ for a narrow line. This confirms the numerical results found in Section 3. The corresponding values for $\bar{E}_\kappa = \langle p^2 \rangle/2m$ are plotted in Fig. 7. They range from $7\hbar\Gamma/40$ for a broad line to $0.53E_r$ for a narrow line.

Finally, we can mention an interesting point that was pointed out to us by Phillips and co-workers, who first obtained this result by using a Monte Carlo approach to this problem[19]; it concerns the large $|\bar{\delta}|$ variation of $\bar{E}_\kappa$ (see Fig. 6). We see that for large $|\bar{\delta}|$, $\bar{E}_\kappa$ increases linearly with $|\bar{\delta}|$, as one would expect from the limit (4.9), but it remains below the semiclassical limit $7\hbar|\bar{\delta}|/40$. This can be understood by a simple reasoning. First, we note that for very large $|\bar{\delta}|$, an expansion such as the one shown in expressions (4.7) and (4.8) is valid, even for narrow atomic lines. In this case, the Doppler shift kp/m is indeed small compared with $|\bar{\delta}|$. In

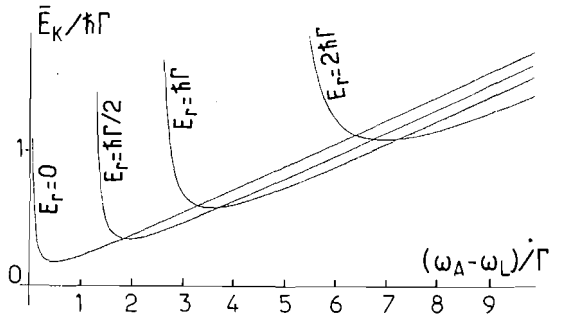

Fig. 6. Variations (for $\Omega \ll \Gamma$) of the stationary kinetic energy $\bar{E}_\kappa$ with detuning δ for various recoil shifts. The curve with $E_r = 0$ represents the predictions of usual semiclassical molasses theory [Eq. (4.9)].

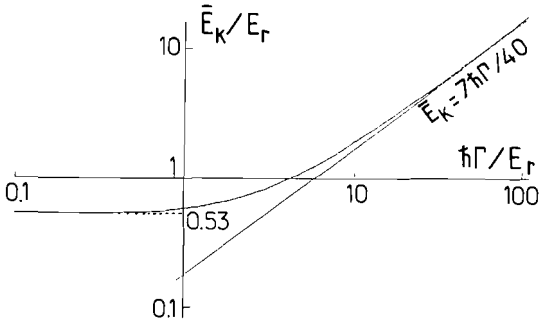

Fig. 7. Variations for $\Omega \ll \Gamma$ of the stationary kinetic energy $\bar{E}_\kappa$ with the ratio $\hbar\Gamma/E_r$. The detuning is always chosen in order to minimize $\bar{E}_\kappa$.

order to obtain a more accurate expression than the semiclassical result (4.9), we improve expansions (4.7) and (4.8) in the following way:

$$\gamma_-(p) - \gamma_+(p) \simeq -\frac{\Gamma\Omega^2\bar{\delta}kp/m}{(\bar{\delta}^2+\Gamma^2/4)^2}(1+Ap^2),$$

$$\gamma_-(p) + \gamma_+(p) \simeq \frac{\Gamma\Omega^2/2}{\bar{\delta}^2+\Gamma^2/4}(1+Bp^2), \tag{4.13}$$

where the two coefficients A and B are obtained from Eq. (3.7):

$$A = \frac{k^2}{m^2}\frac{2\bar{\delta}^2-\Gamma^2/2}{(\bar{\delta}^2+\Gamma^2/4)^2}, \tag{4.14}$$

$$B = \frac{k^2}{m^2}\frac{3\bar{\delta}^2-\Gamma^2/4}{(\bar{\delta}^2+\Gamma^2/4)^2}. \tag{4.15}$$

They are both positive for large $\bar{\delta}$. $A > 0$ means that the force f around $p = 0$ is larger (in modulus) than its tangent in $p = 0$. $B > 0$ means that an atom with nonzero momentum is more likely to be excited than an atom at rest. We now put expansions (4.13) into Eq. (4.5), and we obtain

$$\bar{E}_\kappa = (\bar{E}_\kappa)_{\rm cl} - 2m(3A-B)(\bar{E}_\kappa)_{\rm cl}^2, \tag{4.16}$$

where we note $(\bar{E}_\kappa)_{\rm cl}$, the semiclassical result obtained in Eq. (4.9), and assume that the stationary distribution for $\pi_g(p)$ is close to a Gaussian so that $\langle p^4\rangle \simeq 3(\langle p^2\rangle)^2$. Inserting the explicit values for A and B into Eq. (4.6), we obtain for large $|\bar{\delta}|$

$$\bar{E}_\kappa \simeq (\bar{E}_\kappa)_{\rm cl} - \frac{147}{400}E_r. \tag{4.17}$$

This result can be recovered by use of the exact result [Eq. (B16)] from an asymptotic expansion in $1/\bar{\delta}$.

To sum up, the difference between $\bar{E}_\kappa$ and $(\bar{E}_\kappa)_{\rm cl}$ is due to two effects. First, the force acting on a moving atom is actually larger than the one we would calculate from $p(df/dp)_{p=0}$ (coefficient $A > 0$). Second, momentum diffusion is larger for moving atoms (coefficient $B > 0$). For large δ, we found a decrease of $\bar{E}_\kappa$ with respect to $(\bar{E}_\kappa)_{\rm cl}$. This means that the effect of the extra diffusion compensates only partially for the effect of the extra cooling ($3A > B$).[20]

B. Connection with Semiclassical Treatment: an Approximate Expression for $\pi_g(p)$

We now turn to the problem of connecting our treatment to semiclassical ones, based on a Fokker–Planck equation approach and leading to a Gaussian momentum distribution in the stationary state. Our starting point will be Eqs. (4.1)–(4.3), valid in the low-intensity limit.

We begin by expanding Eq. (4.2) in terms of $\hbar k$; this expansion is valid as long as $\pi_\pm(p)$ do not vary too greatly on the scale $\hbar k$. For the case of broad lines, this is certainly valid for any p, whereas for the case of narrow lines, this is true only when p is large compared with $\hbar k$. In the latter case, we then expect to find the correct asymptotic behavior of $\pi_\pm(p)$ or $\pi_g(p)$, but our results should not be applied in the range $|p| \lesssim \hbar k$. Coming back to the definition of $\bar{\pi}_\pm$ [Eq. (2.19)], we find that

$$\begin{aligned}\bar{\pi}_\pm(p \mp \hbar k) &= \int_{-\hbar k}^{\hbar k} dp' \mathcal{N}(p')\pi_\pm(p+p' \mp \hbar k) \\ &= \pi_\pm(p) \mp \hbar k\left(\frac{\partial\pi_\pm}{\partial p}\right)(p) \\ &\quad + \frac{7\hbar^2k^2}{10}\left(\frac{\partial^2\pi_\pm}{\partial p^2}\right)(p) + \ldots,\end{aligned} \tag{4.18}$$

where we used relation (4.6). Inserting this result into Eq. (4.2), we obtain a Fokker–Planck-type equation with the momentum-dependent force and diffusion coefficient equal to the ones deduced from Eq. (4.5):

$$\frac{\partial}{\partial p}G(p) = 0, \tag{4.19}$$

with

$$G(p) = \pi_-(p) - \pi_+(p) + \frac{7\hbar k}{10}\frac{\partial}{\partial p}[\pi_-(p) + \pi_+(p)]. \tag{4.20}$$

The value of G in $p = \pm\infty$ is zero, so that $G(p)$ is null for any p. If we now replace $\pi_\pm(p)$ with their expression in terms of $\pi_g(p)$, we obtain a first-order differential equation in $\pi_g(p)$, which gives after integration

$$\pi_g(p) = \pi_0\frac{[\Gamma^2/4 + (\bar{\delta}-kp/m)^2][\Gamma^2/4+(\bar{\delta}+kp/m)^2]}{(\Gamma^2/4+\bar{\delta}^2+k^2p^2/m^2)^\alpha}, \tag{4.21}$$

where π_0 is a normalizing coefficient and the exponent α is given by

$$\alpha = 1 - \frac{10\bar{\delta}}{7\hbar k^2/m}. \tag{4.22}$$

For a narrow line, the result (4.21) is only in qualitative agreement with the exact results found numerically in Section 3 for the stationary distribution of $\pi_g(p)$ and also for the rms momentum $\langle p^2\rangle$ found in Subsection 4.A. On the other hand, it gives back exactly the convergence condition of $\int p^{2n}\pi_g(p)dp$, ensuring a finite value for the average value $\langle p^{2n}\rangle$ [see expression (4.10)]. This convergence condition is indeed governed by the large p behavior of $\pi_g(p)$ and $\pi_\pm(p)$, for which expansion (4.18) is valid.

For a broad line, expression (4.21) can be simplified in taking the limit of an infinitely heavy atom ($m \to \infty$, so that $\hbar k^2/m\Gamma \to 0$) while keeping constant the linewidth Γ, the detuning $\bar{\delta}$, and the atomic kinetic energy $E_\kappa = p^2/2m$. The numerator of Eq. (4.21) is immediately found to tend toward the constant value $(\bar{\delta}^2+\Gamma^2/4)^2$, while the calculation of the limit of the denominator requires some more care. First we write

$$(\Gamma^2/4+\bar{\delta}^2+k^2p^2/m^2)^\alpha = \exp[\alpha\ln(\Gamma^2/4+\bar{\delta}^2+k^2p^2/m^2)]. \tag{4.23}$$

Then we expand

$$\ln(\Gamma^2/4+\bar{\delta}^2+k^2p^2/m^2) = \ln(\Gamma^2/4+\bar{\delta}^2) + \frac{k^2p^2/m^2}{\bar{\delta}^2+\Gamma^2/4} + \ldots. \tag{4.24}$$

The first term of the right-hand side is a constant that

must be incorporated in π_0, while the second term of Eq. (4.24) multiplied by α tends to the limit $E_\kappa\bar{\delta}/(\bar{\delta}^2+\Gamma^2/4)$. We therefore obtain the well-known result for broad lines

$$\pi(p)=\tilde{\pi}_0\exp\left(-\frac{E_\kappa}{2\bar{E}_\kappa}\right), \tag{4.25}$$

with $E_\kappa=p^2/2m$ and where $\bar{E}_\kappa$ is given in Eq. (4.9).

In conclusion, Eq. (4.21) appears to be a convenient way to evaluate easily and with a good approximation expressions involving the stationary distribution $\pi_g(p)$ for both narrow and broad lines.

5. CONCLUSION

We have presented in this paper a full quantum method to study the limit of Doppler cooling. This method uses the concept of families corresponding to a given momentum p.[12-14] This method is well suited to the situation studied in this paper, where one-dimensional cooling is produced by two σ_+ and σ_- polarized counterpropagating waves. Conservation of angular momentum prevents coherent redistribution of photons between the two waves, which in turn makes the density-matrix evolution particularly simple when it is written in the family basis.

The method presented here is valid for any ratio between the recoil energy E_r and the natural width $\hbar\Gamma$. It therefore establishes a link between the semiclassical regime $E_r\ll\hbar\Gamma$, which is usually studied by using a Fokker–Planck analysis based on an expansion in terms of the small parameter $\hbar k/\sqrt{p^2}$, and the quantum regime $E_r\gtrsim\hbar\Gamma$. In this quantum regime, we found that the rms momentum is of the order of $\hbar k$. A Fokker–Planck approach cannot in this case give with good precision the complete velocity distribution. However, we showed that it leads to the good asymptotic behavior of the stationary velocity distribution.

We found that this quantum treatment leads to results similar to the ones obtained by a Monte Carlo treatment of the process. The Monte Carlo treatment was performed in the rate-equation approximation. We believe that this result is specific to the cooling of a V system, which does not involve any long-lived coherences in the ground state; a simple Monte Carlo approach could not, for example, give an account of the phenomenon of cooling by coherent population trapping recently discovered in a Λ system. On the other hand, the possibility of describing Doppler cooling by a Monte Carlo approach is important: Monte Carlo methods are indeed the only available methods in practice when the system gets more complicated, i.e., cooling a narrow atomic line with a broadband laser,[17] three-dimensional Doppler cooling,[19] and so forth.

Finally, we emphasize that the family method could be applied to any atomic transition $J_g\to J_e$ (with $J_e=J_g$ or $J_g\pm1$) irradiated with two counterpropagating σ_+ and σ_- laser waves. For instance, for $J_g\neq0$, $J_e=J_g+1$, and for a broad line, Doppler cooling is reinforced by polarization gradient cooling, which lowers the achievable temperature from $\hbar\Gamma$ to a value limited only by E_r.[7] Because of this very low temperature, a Fokker–Planck analysis is no longer applicable, while the family method remains valid and offers a theoretical way to determine the limiting temperature.[10]

APPENDIX A: SPONTANEOUS EMISSION IN THE FAMILY METHOD

The goal of Appendix A is to determine the evolution resulting from spontaneous emission of the nine functions $\pi_g(p)$, $\rho_{+g}(p)$, ... defined in Eqs. (2.2). We start with the master equation giving the evolution of the density operator ρ resulting from spontaneous-emission processes (see, e.g., Ref. 4)

$$\begin{aligned}(d\rho/dt)_{S.E.}=&-\frac{\Gamma}{2}[(\Delta^+\cdot\Delta^-)\rho+\rho(\Delta^+\cdot\Delta^-)]\\&+\frac{3\Gamma}{8\pi}\int d^2\Omega\sum_{\epsilon\perp\mathbf{n}}(\Delta^+\cdot\epsilon)^+\exp(-ik\mathbf{n}\cdot\mathbf{R})\rho\\&\times\exp(ik\mathbf{n}\cdot\mathbf{R})(\Delta^+\cdot\epsilon).\end{aligned} \tag{A1}$$

$\mathbf{R}$ is the position operator of the atomic center of mass, acting only on external variables, and Δ^- and Δ^+ are the lowering and raising parts of the reduced atomic-dipole operator

$$\begin{aligned}\Delta^-&=|g\rangle\langle e_-|u_-+|g\rangle\langle e_+|u_++|g\rangle\langle e_0|u_z,\\\Delta^+&=(\Delta^-)^+.\end{aligned} \tag{A2}$$

Δ^- and Δ^+ differ from the operators $\mathbf{D}^-$ and $\mathbf{D}^+$ defined in Eqs. (2.10) by the multiplicative factor d (electric-dipole moment of the transition). The first line of Eq. (A1) describes the decrease resulting from spontaneous emission of excited-state populations and coherences and of optical coherences (density-matrix elements between an excited state and the ground state). From the contribution of this first line, one immediately deduces the equations of evolution [Eqs. (2.20)].

We now tackle the problem of determining the equation of evolution of $\pi_g(p)$ [see Eq. (2.17)] from the contribution of the second and third lines of Eq. (A1). This line describes how the ground-state population is fed by spontaneous emission of a fluorescence photon in the solid angle $d\Omega$ around direction $\mathbf{n}$, with energy $\hbar ck$ and polarization $\epsilon\perp\mathbf{n}$. We first take the matrix element of Eq. (A1) between $\langle g,\mathbf{p}|$ and $|g,\mathbf{p}\rangle$. We get

$$\begin{aligned}\left(\frac{\partial}{\partial t}\langle g,\mathbf{p}|\rho|g,\mathbf{p}\rangle\right)_{S.E.}=&\frac{3\Gamma}{8\pi}\int d^2\Omega\\&\times\sum_{\epsilon\perp\mathbf{n}}\langle g,\mathbf{p}+\hbar k\mathbf{n}|(\Delta^+\cdot\epsilon)^+\rho(\Delta^+\cdot\epsilon)|g,\mathbf{p}+\hbar k\mathbf{n}\rangle.\end{aligned} \tag{A3}$$

We now expand the vector ϵ on the basis $u_\pm$, u_z [Eqs. (2.11)]:

$$\epsilon=\epsilon_{+1}u_++\epsilon_{-1}u_-+\epsilon_0u_z, \tag{A4}$$

and we obtain from Eq. (A3) by using $\Delta^+\cdot u_q|g\rangle=|e_q\rangle$

$$\begin{aligned}\left(\frac{\partial}{\partial t}\langle g,\mathbf{p}|\rho|g,\mathbf{p}\rangle\right)_{S.E.}=&\frac{3\Gamma}{8\pi}\sum_{qq'}\int d^2\Omega\\&\sum_{\epsilon\perp\mathbf{n}}\epsilon_q\epsilon_{q'}^*\langle e_{q'},\mathbf{p}+\hbar k\mathbf{n}|\rho|e_q,\mathbf{p}+\hbar k\mathbf{n}\rangle,\end{aligned} \tag{A5}$$

where the sum over q and q' ranges from -1 to $+1$. We now

take the trace of ρ over p_x and p_y in order to get the evolution of $\pi_g(p)$:

$$\left(\frac{\partial \pi_g}{\partial t}\right)_{SE}(p) = \frac{3\Gamma}{8\pi}\sum_{qq'}\int d^2\Omega \sum_{\epsilon\perp n}\epsilon_q\epsilon_{q'}^*,$$

$$\langle e_{q'}, p_z = p + \hbar k\cos\theta|\rho|e_q, p_z = p + \hbar k\cos\theta\rangle, \quad \text{(A6)}$$

where θ represent the polar angle of Ω with respect to the Oz axis. The sum over ϵ gives

$$\sum_{\epsilon\perp n}\epsilon_q\epsilon_{q'}^* = \delta_{qq'} - n_q n_{q'}^*, \quad \text{(A7)}$$

and the integral over the azimuthal angle ϕ of Ω leads to

$$\int_0^{2\pi} d\phi \sum_{\epsilon\perp n}\epsilon_q\epsilon_{q'}^* = \frac{8\pi}{3}\delta_{qq'}N_q(\theta), \quad \text{(A8)}$$

with

$$N_\pm(\theta) = \frac{3}{4}\frac{1+\cos^2\theta}{2},$$
$$N_0(\theta) = {}^3/_4\sin^2\theta. \quad \text{(A9)}$$

We now use as a new variable the component along Oz of the momentum of the fluorescence photon

$$p' = \hbar k\cos\theta. \quad \text{(A10)}$$

We note that the contribution of $q = 0$ to Eqs. (A6) can be omitted since the population of the state $|e_0\rangle$ remains zero at any time. Then finally we get

$$\left(\frac{\partial \pi_g}{\partial t}\right)_{SE}(p) = \Gamma\int_{-\hbar k}^{\hbar k} dp'\mathcal{N}(p')$$
$$\times[\pi_+(p-\hbar k+p') + \pi_-(p+\hbar k+p')], \quad \text{(A11)}$$

with

$$\mathcal{N}(p') = \frac{N_\pm(\theta)}{\hbar k} = \frac{3}{8\hbar k}\left[1+\left(\frac{p'}{\hbar k}\right)^2\right], \quad \text{(A12)}$$

which demonstrates Eq. (2.17).

APPENDIX B: STATIONARY RMS MOMENTUM IN THE LOW-INTENSITY LIMIT

Here we wish to derive the rms momentum $\sqrt{\langle p^2\rangle}$ in the stationary state. We consider the low-intensity limit ($\Omega \ll \Gamma$) so that this rms stationary momentum is actually given by the average of p^2 in the ground-state momentum distribution $\pi_g(p)$:

$$\langle p^2\rangle \simeq \langle p^2\rangle_g = \frac{\int dp p^2\pi_g(p)}{\int dp\pi_g(p)}. \quad \text{(B1)}$$

It is useful from a practical point of view to work with dimensionless quantities. Let us define the reduced atomic momentum $q = p/\hbar k$ ($\hbar k$ is expected to be the smallest scale of momentum in the stationary atomic distribution) and the reduced populations:

$$R_g(q) = \hbar k\pi_g(\hbar kq),$$
$$R_\pm(q) = \hbar k\pi_\pm(\hbar kq). \quad \text{(B2)}$$

We also introduce the two dimensionless parameters

$$D = \frac{\bar\delta}{\hbar k^2/2m} \quad \text{(renormalized detuning measured in units of recoil shift)},$$

$$G = \frac{1}{2}\frac{\bar\delta + i\Gamma/2}{\hbar k^2/2m}, \quad \text{(B3)}$$

so that Eq. (4.1) can be written as

$$\left(\frac{\hbar\Omega}{4E_r}\right)^2 R_g(q) = |G-q|^2R_+(q) = |G+q|^2R_-(q). \quad \text{(B4)}$$

Equation (4.2) describing the stationarity of the external degrees of freedom becomes

$$R_+(q) + R_-(q) = \int_{-1}^{+1} dq'\bar{\mathcal{N}}(q')[R_+(q+q'-1) + R_-(q+q'+1)], \quad \text{(B5)}$$

where

$$\bar{\mathcal{N}}(q') = {}^3/_8(1+q'^2) \quad \text{(B6)}$$

is the reduced dipole radiation pattern of spontaneous emission. Finally, the symmetry of the stationary state [Eq. (4.3)] leads to

$$R_g(q) = R_g(-q),$$
$$R_+(q) = R_-(-q). \quad \text{(B7)}$$

We now define the average value R_n of $q^n/n!$ in the state $|e_+\rangle$:

$$R_n = \frac{\int dq R_+(q)q^n/n!}{\int dq R_+(q)}. \quad \text{(B8)}$$

The average value of $q^n/n!$ in the state $|e_-\rangle$ is simply equal to $(-1)^nR_n$, according to Eqs. (B7). Using relation (B4), multiplying by q^2, and integrating over q, we can relate $\langle p^2\rangle_g$ to the coefficients R_n with $n \leq 4$:

$$\langle p^2\rangle_g = \hbar^2k^2\frac{4!R_4 - 3!DR_3 + 2!|G|^2R_2}{2!R_2 - DR_1 + |G|^2}. \quad \text{(B9)}$$

We now calculate R_n recurrently up to $n = 4$. The first recursive relation comes from the parity of $R_g(q)$ [Eqs. (B7)]: the average value of p^{2n-1} in the ground state is zero, which can be written in terms of R_n using Eq. (B4) as

$$(2n+1)R_{2n+1} - DR_{2n} + \frac{|G|^2}{2n}R_{2n-1} = 0. \quad \text{(B10)}$$

The second relation comes from the Eq. (B5), which gives after a multiplication by q^{2n+2} and integration over q

$$\sum_{j=0}^{2n+1} R_jL_{2n-j+2} = 0, \quad \text{(B11)}$$

where we put

$$L_n = \frac{1}{n!}\int_{-1}^{+1}(1+q')^n \bar{\mathcal{N}}(q')\mathrm{d}q'. \tag{B12}$$

The coefficients L_n are simply related to the dipole emission pattern. We get, for instance, $L_1 = 1, L_2 = 7/10, \ldots$. Combining Eqs. (B10) and (B11), we now get a succession of 2×2 systems giving R_{2n} and R_{2n+1} in terms of R_k with $k < 2n$:

$$(2n+1)R_{2n+1} - DR_{2n} = -\frac{|G|^2}{2n}R_{2n-1},$$

$$R_{2n+1} + L_2 R_{2n} = -\sum_{j=0}^{2n-1} R_j L_{2n-j+2}. \tag{B13}$$

On the other hand, relation (B11) for $n = 0$ provides the initial condition

$$R_1 = -L_2. \tag{B14}$$

The calculation of $\langle p^2\rangle$ from Eq. (B9) can now be done in two steps. In the first one, we calculate R_2 and R_3 from the system [Eqs. (B13)] taken for $n = 1$. In the second step, we calculate R_4 from Eqs. (B13) written for $n = 2$. We get, for example,

$$R_2 = \frac{\begin{vmatrix} 3 & L_2|G|^2/2 \\ 1 & L_2L_3 - L_4 \end{vmatrix}}{3L_2 + D}. \tag{B15}$$

This result is physically meaningful if R_2 is positive; we checked that this condition implies that the quantity $3L_2 + D$ has to be negative, or equivalently $\bar{\delta} < -(21/20)\hbar k^2/m$. This ensures that $\int p^2\pi_+(p)\mathrm{d}p$ converges or, according to Eq. (B4), that $\pi_g(p)$ can be normalized. More generally, one expects $\int q^{2n}R_+(q)\mathrm{d}q$ to be positive if the determinant of the linear system [Eqs. (B13)] is negative $[(2n+1)L_2 + D < 0]$, which, because of Eq. (B4), ensures that $\int q^{2n-2}R_g(q)\mathrm{d}q$ is finite and positive. This gives the convergence condition (4.10).

By inserting into Eq. (B9) the value of R_2, R_3, and R_4 calculated from the 2×2 linear systems [Eqs. (B13)], we get the atomic rms momentum in the steady state at the low-intensity limit:

$$\langle p^2\rangle = \frac{1}{4}(L_2\hbar k)^2\left[\tilde{D} - 3 + \frac{1+g^2}{\tilde{D}-5} + 24\frac{10\alpha - (\tilde{D}-3)R(\tilde{D},g)}{\tilde{D}-5}\right]. \tag{B16}$$

We used the following notation in Eq. (B16):

$$R(\tilde{D},g) = 4\frac{\alpha[2g^2 + 3(\tilde{D}-2)^2] + 20\beta}{(\tilde{D}-2)[g^2 + (\tilde{D}-2)^2] + 24\alpha} \tag{B17}$$

and made the following quantities appear:

$$\tilde{D} = -D/L_2,$$
$$g = \hbar\Gamma/(2E_rL_2) \tag{B18}$$

and

$$\alpha = 1/3 - (L_2L_3 - L_4)/{L_2}^3,$$
$$\beta = -1/5 + [L_2L_5 - L_6 + ({L_2}^2 - L_3)(L_2L_3 - L_4)]/{L_2}^5. \tag{B19}$$

The momenta L_n are defined in Eq. (B12).

The coefficients α and β depend only on the radiation pattern $\bar{\mathcal{N}}(q')$ of spontaneous emission along Oz axis. In the case of a purely longitudinal or purely transversal spontaneous emission with respect to the Oz axis, they are both zero. In the real physical case [see Eq. (B6) for $\bar{\mathcal{N}}(q')$], α and β are positive and less than 3×10^{-2}. By neglecting in Eq. (B16) all the terms involving α and β, we find for the mean kinetic energy the approximate formula

$$\bar{E}_\kappa \simeq \frac{1}{4}{L_2}^2E_r\left(\tilde{D} - 3 + \frac{1+g^2}{\tilde{D}-5}\right). \tag{B20}$$

The absolute minimum of the approximation of $\bar{E}_\kappa$ given in formula (B20) is reached in the limit of an ultranarrow line for an optical renormalized detuning [see Eq. (2.8)]

$$\hbar\bar{\delta} = -6L_2E_r = -4.2E_r \tag{B21}$$

and has the value

$$(\bar{E}_\kappa)_{\mathrm{inf}}^{\mathrm{approx}} = {L_2}^2E_r = 0.49E_r. \tag{B22}$$

This must be compared with the exact values given in Section 4 and deduced from Eq. (B16):

$$\hbar\bar{\delta} \simeq -4.45E_r,$$
$$(\bar{E}_\kappa)_{\mathrm{inf}} \simeq 0.53E_r. \tag{B23}$$

ACKNOWLEDGMENTS

We acknowledge many helpful discussions with C. Cohen-Tannoudji, W. Ertmer, J. M. Courty, A. Aspect, and C. Salomon. H. Wallis acknowledges support from the Deutsche Forschung Gemeinschaft under grant ER-113/4-2 and thanks the Laboratoire de Spectroscopie Hertzienne for its hospitality.

We also thank W. D. Phillips and his group for having communicated their results of the Monte Carlo simulation before publication.

The Ecole Normale Superiéure is associated with the Centre National de la Recheche Scientifique (Unité Associée 18) and the Université Pierre et Marie Curie.

* Permanent address, Institut für Angewandte Physik der Universität Bonn, Wegelerstrasse 8, D-5300, Bonn 1, Federal Republic of Germany.

REFERENCES AND NOTES

1. T. W. Hänsch and A. Schawlow, Opt. Commun. **13**, 68 (1975).
2. D. Wineland and H. Dehmelt, Bull. Am. Phys. Soc. **20**, 637 (1975).
3. See, e.g., S. Stenholm, Rev. Mod. Phys. **58**, 699 (1986).
4. J. Dalibard and C. Cohen-Tannoudji, J. Phys. B **18**, 1661 (1985).
5. S. Chu, L. Hollberg, J. E. Bjorkholm, A. Cable, and A. Ashkin, Phys. Rev. Lett. **55**, 48 (1985).
6. P. Lett, R. Watts, C. Westbrook, W. D. Phillips, P. Gould, and H. Metcalf, Phys. Rev. Lett. **61**, 169 (1988).

7. J. Dalibard, C. Salomon, A. Aspect, E. Arimondo, R. Kaiser, N. Vansteenkiste, and C. Cohen-Tannoudji, in *Proceedings of the 11th Conference on Atomic Physics, Paris, July 1988*, S. Haroche, J. C. Gay, and G. Grynberg, eds. (World Scientific, Singapore, 1989).
8. S. Chu, D. S. Weiss, Y. Shevy, and P. J. Ungar, in *Proceedings of the 11th Conference on Atomic Physics, Paris, July 1988*, S. Haroche, J. C. Gay, and G. Grynberg, eds. (World Scientific, Singapore, 1989).
9. W. D. Phillips, National Institute of Standards and Technology, Gaithersburg, Maryland 20899 (personal communication, 1988).
10. J. Dalibard and C. Cohen-Tannoudji, J. Opt. Soc. Am. B **6**, 2023 (1989).
11. J. Dalibard, S. Reynaud, and C. Cohen-Tannoudji, J. Phys. B **17**, 4577 (1984).
12. S. Stenholm, Appl. Phys. **15**, 287 (1978).
13. C. Bordé, in *Advances in Laser Spectroscopy*, S. Arecchi and F. Strumia, eds. (Plenum, New York, 1983).
14. A. Aspect, E. Arimondo, R. Kaiser, N. Vansteenkiste, and C. Cohen-Tannoudji, Phys. Rev. Lett. **61**, 826 (1988); J. Opt. Soc. Am. B **6**, 2112 (1989).
15. D. Wineland and W. Itano, Phys. Rev. A **20**, 1521 (1979).
16. R. Blatt, G. Lafyatis, W. Phillips, S. Stenholm, and D. Wineland, Phys. Scr. **T22**, 216 (1988).
17. H. Wallis and W. Ertmer, in *Proceedings of the 11th Conference on Atomic Physics, Paris, July 1988*, S. Haroche, J. C. Gay, and G. Grynberg, eds. (World Scientific, Singapore, 1989); J. Opt. Soc. Am. B. 26, 2111 (1989).
18. This result is apparently in contradiction to the limit derived in Ref. 16. Actually, this limit was obtained by an energy balance in a single absorption–spontaneous-emission cycle, without any reference to the excitation rate. The argument is therefore valid only if the excitation rate is nearly constant with respect to atomic velocity. This condition is violated for the cooling with a broadband laser of Ref. 17, in which the excitation rate for an atom at rest is much smaller than for an atom with a velocity larger than $\hbar k/m$.
19. P. D. Lett, W. D. Phillips, S. L. Rolston, C. E. Tanner, R. N. Watts, and C. I. Westbrook, J. Opt. Soc. Am. B **6**, 2084 (1989).
20. One could be tempted to obtain this result with a simple reasoning dealing only with energy balance in a single-absorption–spontaneous-emission cycle. In such reasoning the probability of absorption $r_\pm$ of one $\sigma_\pm$ photon is obtained from $r_\pm = \gamma_\pm/(\gamma_+ + \gamma_-)$. One would therefore start from $\langle p(r_- - r_+)\rangle = 7\hbar k/10$ instead of Eq. (4.5) and would obtain after a similar algebra $\bar{E}_\kappa = (\bar{E}_\kappa)_{\rm cl} + 147\, E_r/400$ instead of expression (4.17). The error in such simple reasoning lies in the fact that one would neglect the variation with velocity of the time interval between successive cycles. Taking this variation into account correctly enhances the contribution to $\langle p^2\rangle$ of low-velocity atoms and gives back the correct result [expression (4.17)].